

1 Intracellular carbon storage by microorganisms is an overlooked pathway of 2 biomass growth

3

4 Kyle Mason-Jones^{*1,2}, Andreas Breidenbach^{2,3}, Jens Dyckmans⁴, Callum C. Banfield^{2,3}, Michaela A.
5 Dippold^{2,3}

6

7 ^{*1} Department of Terrestrial Ecology, Netherlands Institute of Ecology (NIOO-KNAW), 6708 PB
8 Wageningen, the Netherlands

9 ² Division of Biogeochemistry of Agroecosystems, Georg-August University of Göttingen, 37073
10 Göttingen, Germany

11 ³ Department of Geosciences, Geo-Biosphere Interactions, University of Tübingen,
12 Schnarrenbergstrasse 94-96, 72076 Tübingen, Germany.

13 ⁴ Centre for Stable Isotope Research and Analysis, Georg-August University of Göttingen, 37073
14 Göttingen, Germany.

15 Abstract

16 The concept of microbial biomass growth is central to microbial carbon (C) cycling and ecosystem
17 nutrient turnover. Growth is usually assumed to occur by cellular replication, despite
18 microorganisms' capacity to increase biomass by synthesizing storage compounds. Here we
19 examined whether C storage in triacylglycerides (TAGs) and polyhydroxybutyrate (PHB) contribute
20 significantly to microbial biomass growth, under contrasting conditions of C availability and
21 complementary nutrient supply. Together these compounds accounted for $19.1 \pm 1.7\%$ to $46.4 \pm$
22 8.0% of extractable soil microbial biomass, and revealed up to $279 \pm 72\%$ more biomass growth than
23 observed by a DNA-based method alone. Even under C limitation, storage represented an additional
24 $16 - 96\%$ incorporation of added C into microbial biomass. These findings encourage greater
25 recognition of storage synthesis and degradation as key pathways of biomass change and as
26 mechanisms underlying resistance and resilience of microbial communities.

27

28

29 1 Introduction

30 Microbial assimilation of organic resources is a central process in most ecosystems. Soil
31 heterotrophs perform key steps in terrestrial carbon (C) and nutrient cycles, yet how
32 microorganisms use the available organic resources and regulate their allocation to competing
33 metabolic demands remains a subject of research and debate¹⁻³. Microbial assimilation of organic C
34 is often conceptualized as “biomass growth”, which is typically envisioned as an increase in microbial
35 abundance, i.e. replicative growth. However, many microorganisms are capable of storage, defined
36 as the accumulation of chemical resources in particular forms or compartments to secure their
37 availability for future use. Various microbial storage compounds are known, including
38 polyhydroxybutyrate (PHB) and triacylglycerides (TAGs)^{4,5}. PHB storage is only known among
39 bacteria, while TAGs are used by both bacteria and fungi⁶. Accumulation of storage compounds
40 corresponds to an increase in microbial biomass without replication, and therefore represents an
41 alternative pathway for growth that is not usually considered in the C cycle.

42 Conventional methods for measuring soil microbial biomass either require extraction into aqueous
43 solution after chloroform fumigation⁷, thereby excluding hydrophobic storage in PHB and TAGs, or
44 measure biomass proxies such as cell membrane lipids or substrate-induced respiration that are not
45 proportional to storage^{8,9}. This potential shortcoming is shared with more recent DNA-based
46 measures of microbial growth^{10,11}. Biosynthesis of PHB has been demonstrated by compound-
47 specific measurement in soil¹² and TAGs in marine and soil systems show responsiveness to resource
48 supply consistent with a C-storage function^{13,14}. Since “biomass growth” is a cornerstone concept at
49 scales from local ecological stoichiometry to microbially-explicit Earth system models^{15,16}, there is a
50 need to assess how severely the omission of storage may bias our understanding of carbon
51 assimilation and utilisation.

52 Interpretation of storage patterns is facilitated by distinguishing two storage modes, which
53 represent the end-members on a gradient of storage strategies^{6,17}. Surplus storage is the
54 accumulation of resources that are available in excess of immediate needs, at little to no opportunity
55 cost, while reserve storage accumulates limited resources at the cost of other metabolic functions.
56 Surplus storage of C would be predicted under conditions of C oversupply, when replicative growth
57 is constrained by other factors such as nutrient limitation. Reserve storage, on the other hand,
58 predicts that storage may also occur under C-limited conditions. Evidence assembled from pure
59 culture studies confirms the operation of both storage modes among microorganisms^{6,18-20}. Here we
60 experimentally investigate the importance of microbial storage in soil, and show how storage

61 responses to resource supply and stoichiometry can advance our understanding of resource
62 allocation and microbial biomass growth. We hypothesized as follows:

- 63 1) Microbial storage compounds account for a substantial proportion of soil microbial biomass
64 under C-replete, nutrient-limited conditions.
- 65 2) Due to low opportunity costs, surplus storage is likely to be quantitatively more significant at
66 the community scale. Therefore, complementary nutrients will suppress storage compound
67 accumulation in favour of replicative growth.
- 68 3) Microbial biomass growth is substantially underestimated by neglecting intracellular
69 storage.

70 Soil microcosms were incubated under controlled conditions, with C availability manipulated
71 through additions of isotopically labelled (^{13}C and ^{14}C) glucose, which is a common component of
72 plant root exudates and the most abundant product of plant-derived organic matter
73 decomposition²¹. Nutrient supply (N, P, K and S) was manipulated by adding inorganic fertilizers
74 common in agriculture. A fully crossed design included three levels of C addition (zero-C, low-C and
75 high-C; 0, 90 and 400 $\mu\text{g C/g soil}$) and two levels of nutrient supply (no-nutrient and nutrient-
76 supplemented) with nutrients supplemented at a level predicted to enable full C assimilation under
77 the high-C treatment. CO_2 efflux was monitored at regular intervals and microcosms were harvested
78 after 24 and 96 hours to determine microbial biomass (by chloroform fumigation-extraction),
79 dissolved organic carbon (DOC), dissolved nitrogen (DN) and the storage compounds PHB and TAGs.
80 In parallel, a set of smaller microcosms (0.5 g soil) was incubated under otherwise identical
81 conditions to measure microbial growth as the incorporation of ^{18}O from H_2^{18}O into DNA¹¹. This
82 method measures the turnover of the microbial population and therefore captures replicative
83 growth better than tracing of specific C substrates³. Together these form the first integrated
84 observations of heterotrophic microbial biomass, growth and storage in a natural microbiome,
85 revealing the importance of storage as a resource-use strategy in response to environmental
86 resource supply and element stoichiometry.

87

88 2 Results and discussion

89 2.1 Microbial nutrient status and CO_2 efflux

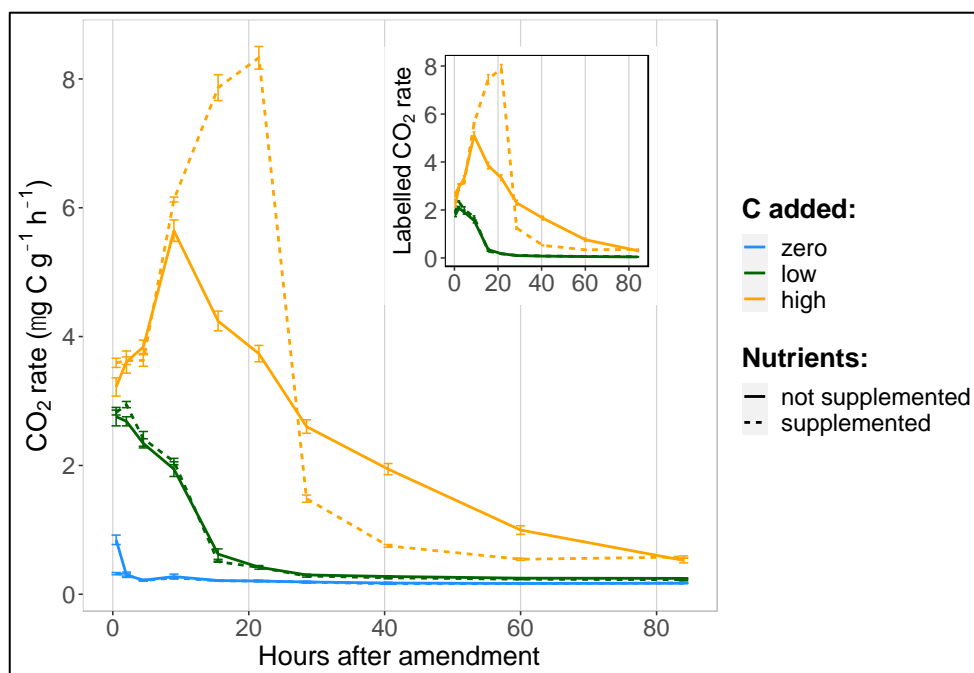
90 Patterns of soil respiration were in general agreement with past studies of low-molecular weight
91 organic substance utilization in soil²²⁻²⁴, and provide interpretive insight into the resource
92 constraints during storage compound synthesis and degradation.

93 Glucose addition stimulated large increases in CO₂ efflux (Figure 1), primarily derived from glucose
94 mineralization (Figure 1, inset). Nutrient supplementation barely affected CO₂ efflux rates from the
95 zero- or low-C additions and for none of these treatments was N availability (measured as dissolved
96 nitrogen) significantly reduced relative to the control at 24 h (Supplementary Figure S1). Thus, C
97 limitation dominated in the zero- and low-C treatments throughout the experimental period,
98 irrespective of nutrient additions.

99 With high-C addition, CO₂ efflux rates under the two nutrient levels diverged strongly after 12 hours,
100 with the no-nutrient treatment declining steadily from 12 h until the end of the experiment. This
101 early decline in mineralization was consistent with the onset of nutrient limitation, after microbial
102 growth on the added glucose had depleted easily available soil nutrients (Supplementary Figure S2).
103 This depletion was reflected in suppressed dissolved nitrogen after 24 h, with only 35.8 – 62.5% of
104 the zero-C, no-nutrient control (family-wise 95% confidence interval; Supplementary Figure S1) and
105 a further decline to 96 h. Nutrient limitation was accompanied by an accumulation of highly-labelled
106 DOC at 24 h in the soil solution, reflecting unused glucose or soluble by-products in an amount 19.6
107 $\pm 2.1\%$ of the original C addition (mean \pm standard deviation; Supplementary Figure S3). High C
108 addition without supplementary nutrients resulted in rapid mineralization at first, but nutrient
109 limitation set in within 12 hours and continued for the remaining experimental period.

110 Nutrient addition had a strong effect in combination with high-C supply: it accelerated glucose
111 mineralization until 24 hours after addition (Figure 1), after which CO₂ efflux dropped precipitously
112 to below that of the high-C, no-nutrient treatment. Dissolved N decreased only moderately over 24 h
113 (56.2 – 97.9% of control, despite the added nutrients). DOC at 24 h was far lower than in the
114 absence of added nutrients, with no further change to 96 h, despite higher N availability (Cohen's d
115 $\gg 1$, family-wise $p < 0.001$ for both), indicating that the microbial community had depleted the
116 added C and re-entered C-limited conditions. Therefore, high C addition with supplementary
117 nutrients maintained rapid C mineralization through the first 24 hours, but glucose depletion then
118 reasserted C-limitation for the rest of the experimental period.

119



120

121 **Figure 1:** Time-series of the CO₂ efflux from soil microcosms following addition of a readily
 122 degradable ¹³C-labelled carbon source (glucose at 0, 90 and 400 μg C g⁻¹ soil) with or without mineral
 123 nutrient supply (N, P, K, S). Inset shows only CO₂ derived from the added glucose in μg C g⁻¹ h⁻¹. Each
 124 point plots the average rate of CO₂ efflux at the mid-point of the sampling interval, with error bars
 125 showing standard deviation (n = 4).

126

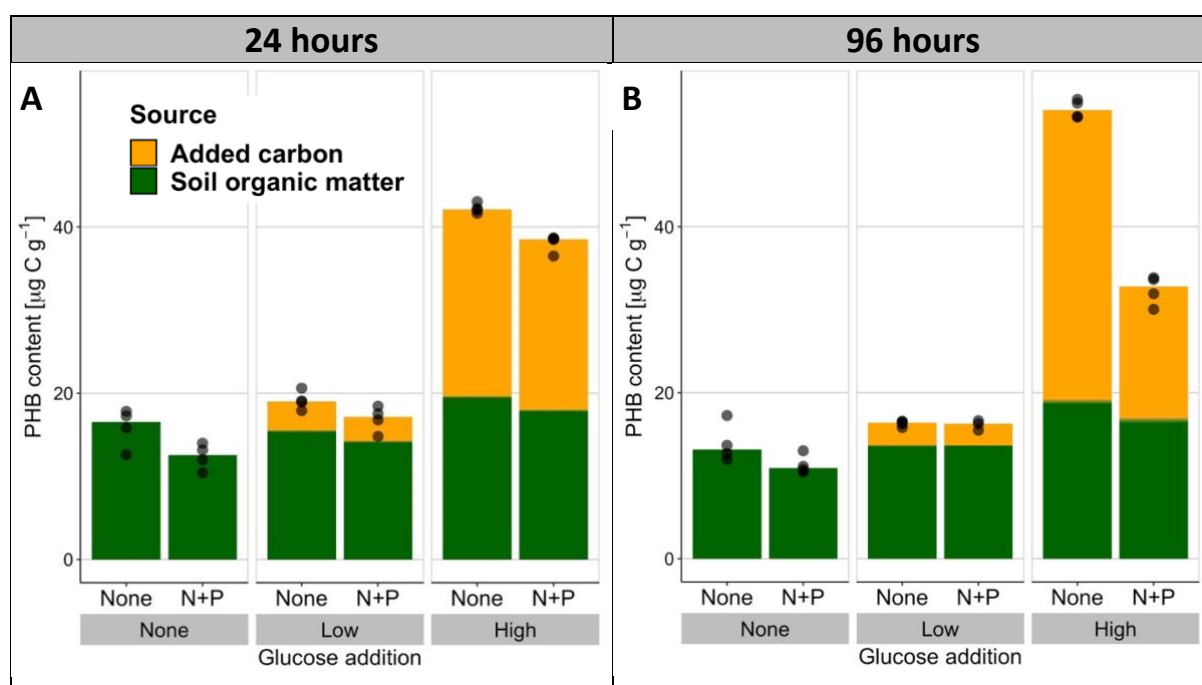
127 2.2 Presence and synthesis of microbial storage compounds

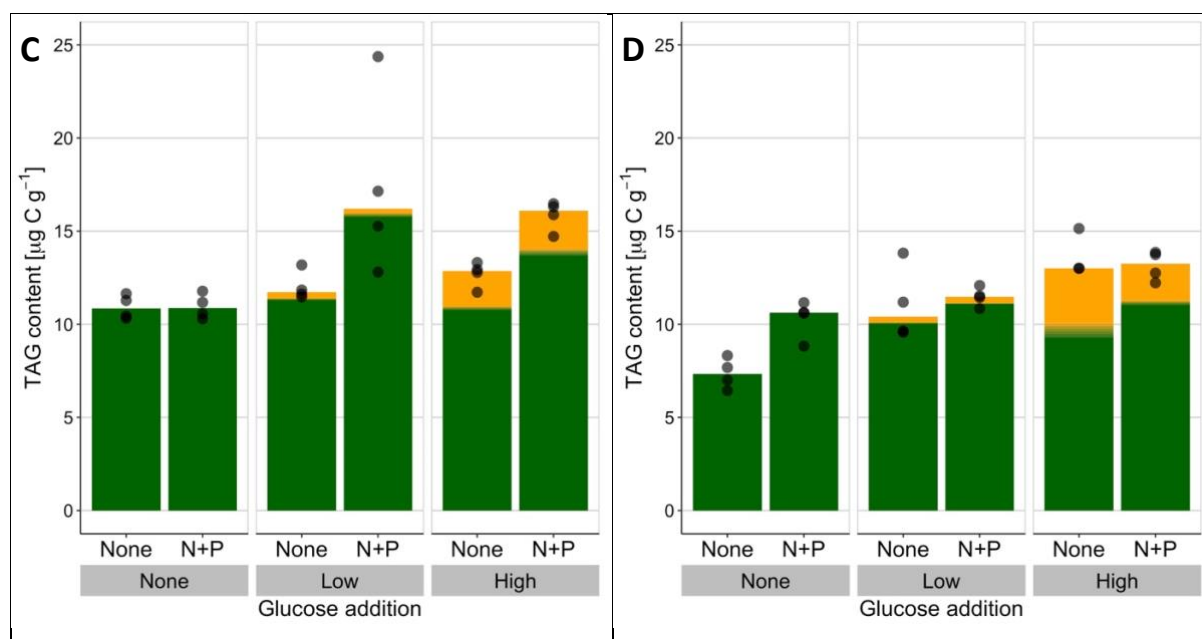
128 PHB and TAGs were both found in the control soil (zero-C, no nutrients after 24 h; Figure 2, A&C),
 129 together representing a pool $24.7 \pm 2.5\%$ (mean \pm standard deviation) as large as the extractable
 130 microbial biomass (Figure S2). This ratio ranged from $19.1 \pm 1.7\%$ to $46.4 \pm 8.0\%$ over all treatments,
 131 indicating that storage is a significant pool of biomass not only under C-replete conditions, as
 132 hypothesized, but even when C availability is limited. Storage equivalent to a substantial proportion
 133 of biomass offers a resource for regrowth following disturbance, indicating a potential role of
 134 storage in supporting resilience of this soil microbial community. Furthermore, most common
 135 measures of soil microbial biomass rely on proxies such as soluble carbon after chloroform
 136 fumigation, which do not capture this biomass component. This suggest that microbial biomass C
 137 may be widely underestimated in soil.

138 The two storage compounds were both responsive to the supply of C and complementary nutrients,
 139 but with very different behaviours. At both timepoints, the low input of C stimulated only a
 140 moderate increase in total PHB, irrespective of nutrient supply. In contrast, high C input stimulated a
 141 large increase in PHB, particularly when not supplemented with nutrients (a 308% increase over
 142 control at 96 h, with Hodges-Lehmann median difference of $36.0 - 42.9 \mu\text{g C g}^{-1}$). Nutrient supply

143 significantly suppressed PHB storage, even in the absence of added C (nutrient main effect, robust
 144 ANOVA of medians 24 h: $F_{(1,\infty)} = 35$, $p < 0.001$; 96 h: $F_{(1,\infty)} = 275$, $p < 0.001$). Assimilation of glucose C
 145 into new PHB continued between 24 and 96 h under the nutrient-limited conditions of the high-C,
 146 no-nutrient treatment (Hodges-Lehmann median difference of $10.2 - 13.3 \mu\text{g C g}^{-1}$, 95% confidence
 147 interval), while in contrast the increasing C limitation of the high-C, nutrient-supplemented
 148 treatment after 24 h induced degradation of PHB during this late incubation period (median
 149 reduction of $2.7 - 8.6 \mu\text{g C g}^{-1}$). The PHB storage pool therefore responded dynamically to shifts in
 150 resource stoichiometry on a timescale of hours to days, with changes as expected from a surplus
 151 storage strategy. Dynamic build-up of storage under conditions of surplus and mobilisation under
 152 scarcity mirrors diurnal storage oscillations observed in the ocean¹⁴ as well as patterns described in
 153 pure culture²⁵. This study provides the first confirmation of such microbial storage dynamics in a
 154 terrestrial ecosystem. At the end of the incubation, stored C was sufficient to completely support
 155 basal respiration for 109 – 347 h (depending on the treatment), which could be a crucial resource for
 156 withstanding starvation or other stress. Much longer periods would be envisaged if accompanied by
 157 strong downregulation of energy use in response to the stress²⁶. Thus, the resource buffer provided
 158 by storage could help microorganisms in terrestrial ecosystems overcome resource fluctuations and
 159 support short-term resistance against environmental disturbance⁶.

160





161

162 **Figure 2:** Storage compounds PHB (above, A, B) and TAGs (below, C, D) in soil following addition of a
 163 readily degradable, ^{13}C -labelled carbon source (glucose at 0, 90 and 400 $\mu\text{g C g}^{-1}$ soil) with or without
 164 mineral nutrient supply (N, P, K, S). Soil was sampled after 24 h (left) and 96 h (right). The source of the
 165 stored C is shown in contrasting colours as determined by isotopic composition, with uncertainty
 166 in relative composition shown as shading of the colours around the mean of composition (shading
 167 corresponds to \pm standard deviation, $n = 4$, except for 1 treatment in each of TAGs and PHB where
 168 $n = 3$).

169

170 Storage of TAGs was enhanced by C input (Figure 2, C&D), but its response to resource stoichiometry
 171 differed greatly from PHB. Over 24 h, nutrient supplementation stimulated more TAG accumulation,
 172 rather than suppressing it (main nutrient effect $F_{(1,\infty)} = 10.8$, $p = 0.001$ and nutrient:glucose
 173 interactions between zero-C and the two C-supplemented treatments, both $p < 0.01$), while over 96
 174 h nutrient supply had little effect with C addition and increased TAGs when C was not added (95%
 175 confidence interval for median difference 0.5 – 4.7 $\mu\text{g C g}^{-1}$). The TAG response to C and nutrient
 176 supply over 96 h resembled changes in extractable microbial biomass (Supplementary Figure S2),
 177 which was increased by C supply but not significantly enhanced by nutrients (ANOVA main effect of
 178 C supply at 96 h: $F_{(2,17)} = 8.0$, $p = 0.003$). Therefore, unlike PHB, TAG synthesis was not stimulated by
 179 a stoichiometric surplus of available C, suggesting a reserve storage function for this compound.
 180 Notably, the relative allocation of glucose C between PHB and TAG remained relatively constant
 181 (glucose-derived PHB:TAG ranged 7.0 – 11.5 across all treatments) because the C source used for
 182 TAG biosynthesis varied more strongly than total TAG levels in response to C supply. This
 183 corroborates a reserve storage function of TAG, with total storage synthesis regulated independently
 184 of C supply and drawing on whichever C resources are available, whether glucose- or soil-derived.

185

186 A reserve storage role for TAG contrasts with an earlier report that fungal TAG accumulation in a
187 forest soil was largely eliminated by complementary nutrient supply¹³, with the difference possibly
188 attributable to the much higher amounts of C provided in that experiment (16 mg glucose-C g⁻¹). In
189 our experiment C was traced into both bacterial (16:1ω7) and fungal (18:2ω6,9) TAGs
190 (Supplementary material Figures S4, S5 and S6). The fungal biomarker 18:2ω6,9 was only a minor
191 contributor to TAG incorporation in the current experiment, yet even this fungal TAG was not
192 suppressed by nutrient addition. Our results indicate that both fungi and bacteria employed TAGs as
193 a reserve storage form, with overall levels of TAG storage more closely linked to replicative growth
194 than to resource stoichiometry.

195

196 In summary, the response of PHB storage to different C and nutrient conditions was largely
197 consistent with the hypothesized surplus storage mode. In contrast, patterns of TAG storage were
198 better characterized by the reserve storage mode. Since some bacterial taxa can utilize both PHB
199 and TAGs^{27,28}, the question arises whether these compounds fulfil different storage functions in
200 individual organisms, or whether the different responses emerge at a community scale, with each
201 compound consistently preferred by a different set of microbial taxa, following divergent storage
202 strategies. In the latter case, storage traits may prove useful contributions to microbial trait-based
203 frameworks as proxies of an organism's resource allocation strategy.

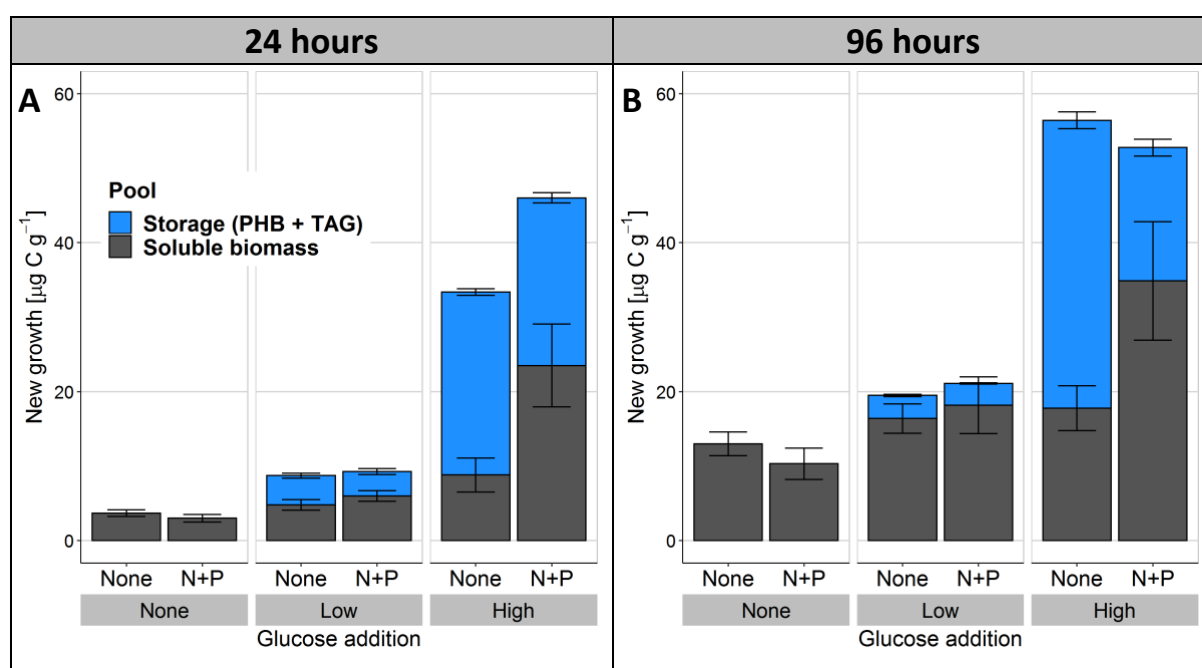
204

205 2.3 Microbial storage as a component of biomass growth

206 The incorporation of C into soil microbial biomass is an essential step in the terrestrial C cycle, and
207 appropriate estimates of these flows are required for C modelling and environmental management.
208 We performed a parallel experiment to measure microbial growth using ¹⁸O incorporation into
209 DNA¹¹. This method is calibrated to units of carbon content based on extractable biomass from the
210 chloroform fumigation-extraction method, and therefore does not capture hydrophobic PHB or TAG
211 storage. We compared the ¹⁸O-based measure of growth with the net incorporation of isotopically
212 labelled glucose carbon into storage compounds (Figure 3). This provides a comparison of magnitude
213 using a lower bound for storage synthesis by neglecting the biosynthesis of storage from other C
214 sources and any degradation of labelled storage prior to measurement. Furthermore, only two
215 storage forms were measured here, whereas other microbial storage compounds are also known⁶.
216 Storage comprised up to 279 ± 72% more biomass growth than observed by the DNA-based method

217 (mean \pm standard deviation for the high-C, no-nutrient treatment at 24 h, Figure 3A). Even under
 218 conditions of C limitation, this storage growth represented an additional 16 – 96% incorporation of C
 219 into biomass. Intracellular storage evidently plays a quantitatively significant role in microbial
 220 assimilation of C under a broad range of stoichiometric conditions, and biomass growth would be
 221 substantially underestimated by neglecting storage. As microbial growth is a central variable in
 222 microbially-explicit models of the carbon cycle²⁹, the substantial scale of storage also encourages a
 223 reassessment of model inputs and interpretation of results wherever short-term measurements or
 224 dynamic changes are involved.

225



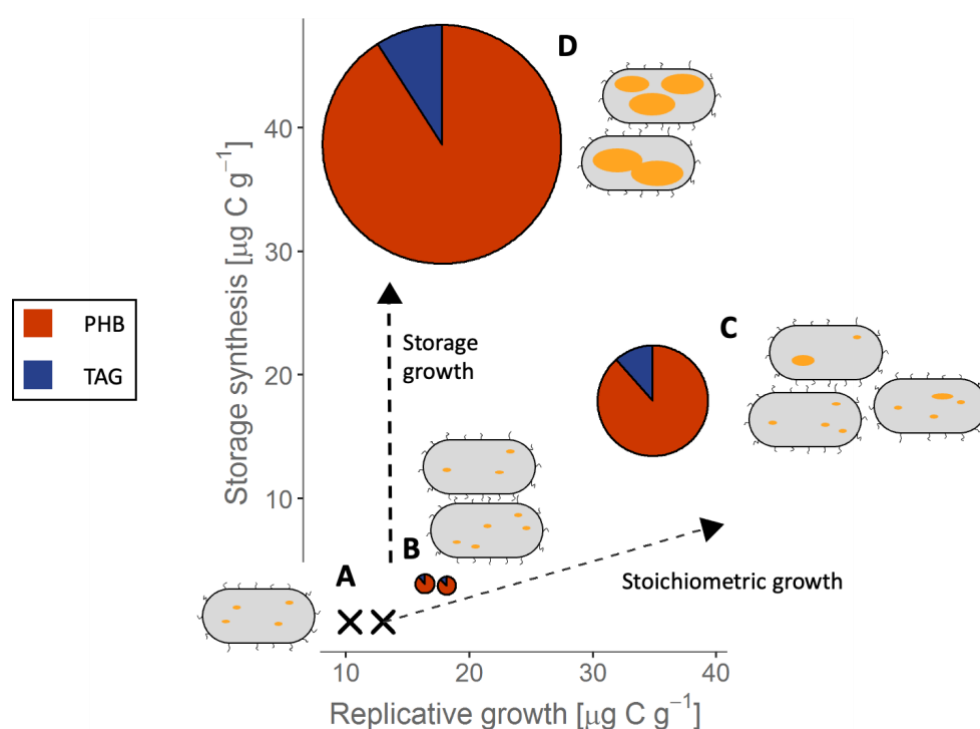
226 **Figure 3:** Conservative estimation of new storage biosynthesis in comparison to DNA-based
 227 microbial growth reveals storage as a substantial, overlooked component of biomass growth in soil.
 228 Here ¹³C-labelled storage compound synthesis (PHB and TAGs) and DNA-based growth
 229 (incorporation of ¹⁸O) were measured in soil over 24 (A) and 96 hours (B) following addition of a
 230 readily degradable, ¹³C-labelled carbon source (glucose at 0, 90 and 400 µg C g⁻¹ soil) with or without
 231 mineral nutrient supply (N, P, K, S). Error bars represent standard deviations in each component of
 232 the stacked bar (n = 4).

233

234 “Microbial biomass growth” is frequently understood as synonymous with an increase in individuals,
 235 in other words, the replicative growth of microbial populations. However, the incorporation of C into
 236 storage compounds represents an alternative growth pathway (Figure 4), which differs from
 237 replicative growth in crucial ways. Models of microbial growth typically assume that increases in
 238 biomass match the elemental stoichiometry of the total biomass (the assumption of stoichiometric
 239 homeostasis³⁰), and therefore implement overflow respiration of excess C under conditions of C

240 surplus³¹. However, substantial incorporation of C into otherwise nutrient-free PHB and TAG clearly
 241 does not follow whole-organism stoichiometry. Growth in storage therefore increases total biomass
 242 under stoichiometrically unbalanced conditions. The short experimental timeframe here is
 243 representative of environmental resource pulse and depletion processes, such as the arrival of a
 244 root tip in a particular soil volume or death and decay of a nearby organism. Storage provides
 245 stoichiometric buffering during such transient resource pulses, which is predicted to increase C and
 246 N retention over the longer term³². By enhancing the efficiency with which microbes incorporate
 247 transient resource pulses and supporting metabolic activity through periods of resource scarcity,
 248 storage can contribute to resistance and resilience of microbial communities facing environmental
 249 disturbances.

250



251

252 **Figure 4:** Intracellular storage represents an alternative pathway for growth of microbial biomass,
 253 which can be quantitatively substantial but is usually omitted from contemporary discussions. In this
 254 conceptual figure the y-coordinates and radii of the pie charts reflect the measured incorporation of
 255 added C into storage, with pie chart colours showing the contributions of PHB and TAG (× for zero-C
 256 treatments). A microbial population is shown schematically by bacterial cells, with yellow lipid
 257 inclusion bodies representing storage. Without C supply, only low levels of replicative growth occur
 258 (A). Low C additions (with ample nutrients) stimulate replicative growth and limited C incorporation
 259 into storage (B), with proportions of new storage and non-storage biomass staying close to those
 260 predicted by an assumption of constant biomass stoichiometry (dashed line to the right). High C
 261 addition with complementary nutrients stimulates both strong replicative growth as well as
 262 disproportionately large storage synthesis (C) moderately violating the stoichiometric assumption.
 263 However, nutrient limitation switches growth strongly towards storage (D), incorporating C into

264 biomass without proportionate replicative growth. Replicative growth was measured as ^{18}O
265 incorporation into DNA (see also Figure 3).

266

267 These findings encourage greater recognition of storage synthesis and degradation as pathways of
268 microbial biomass change in natural communities, in addition to cellular replication. Accounting for
269 microbial storage as a key ecophysiological strategy can enrich our understanding of microbial
270 resource use and its quantitative contribution to global biogeochemical cycles.

271

272 3 Methods

273 3.1 Experimental design

274 Topsoil (0 – 25 cm) was collected in November 2019 from the Reinshof experimental farm near
275 Göttingen, Germany (51°29'51.0" N, 9°55'59.0" E) following an oat crop. Five samples along a field
276 transect were mixed to provide a single homogenized soil sample. The soil was a Haplic Luvisol, pH
277 5.4 (CaCl_2), C_{org} 1.4%³³. Soil was stored at 4°C prior to sieving (2 mm) and then distributed into
278 airtight 100 mL microcosms in laboratory bottles with the equivalent of 25 g dry soil at 48% of water
279 holding capacity (WHC). Four replicates were prepared for each treatment and sampling timepoint.
280 Microcosms were placed in a climate-controlled room at 15°C and preincubated for one week before
281 adding treatment solutions.

282 Treatment solutions provided glucose as a C source (0, 90 or 400 $\mu\text{g C/g soil}$) in a fully crossed design
283 with added nutrients (combined $(\text{NH}_4)_2\text{SO}_4$ and KH_2PO_4) or a no-nutrient control. Glucose treatments
284 contained uniformly isotopically labelled glucose (3 atom% ^{13}C and 0.19 kBq ^{14}C per microcosm,
285 respectively from Sigma-Aldrich, Munich, Germany and from American Radiolabelled Chemicals,
286 Saint Louis, U.S.A.). The N and P addition was set to be sufficient for the complete utilisation of the C
287 in the high glucose treatment, assuming a C:N:P ratio of 38:5:1 for an agricultural microbial
288 community³⁴ and a C-use efficiency of 50%³⁵. Addition of the treatment solutions raised the soil
289 moisture to 70% of WHC, after which the microcosms were sealed with air-tight butyl rubber septa
290 and their headspace flushed with CO_2 -free synthetic air. Headspace gas was sampled with a 30 mL
291 gas syringe at regular intervals and collected in evacuated exetainers (Labco, Ceredigion, U.K.) for
292 measurement by gas chromatography – isotope ratio mass spectrometry (GC-Box coupled via a
293 Conflo III interface to a Delta plus XP mass spectrometer, all Thermo Fischer, Bremen, Germany).
294 After gas sampling, the headspace in each microcosm was again flushed with CO_2 -free air.

295 Microcosms were harvested 24 and 96 hours after application of the treatment solutions. The soil in
296 each microcosm was thoroughly mixed by hand for 30 sec and subsampled for chemical analysis.

297

298 3.2 Chemical analysis

299 Extractable microbial biomass was measured by chloroform fumigation extraction^{7,36}. Two 5 g
300 subsamples of moist soil were taken from each microcosm. One was immediately extracted by
301 shaking in 20 mL of 0.05 M K₂SO₄ for 1 hour at room temperature, then centrifuged and the
302 supernatant filtered. The other was exposed to a chloroform-saturated atmosphere for 24 hours,
303 after which residual chloroform was removed by repeated evacuation and the fumigated soil was
304 extracted in the same manner as the non-fumigated subsample. Extractable MBC was calculated as
305 the difference in DOC between the fumigated and non-fumigated samples, measured on a Multi N/C
306 2100S analyser (Analytik Jena, Jena, Germany). Glucose-derived MBC was similarly calculated from
307 the difference in radioactivity (¹⁴C) of the extracts as measured on a Hidex 300 SL scintillation
308 counter (TDCR efficiency correction, Hidex, Turku, Finland) using Rotiszint Eco Plus scintillation
309 cocktail (Carl Roth, Karlsruhe, Germany). Dissolved nitrogen was determined as total nitrogen in the
310 extracts of the unfumigated soil.

311 PHB was determined by the method of Mason-Jones et al.¹², using Soxhlet extraction into
312 chloroform followed by acid-catalysed transesterification in ethanol and GC-MS quantification of the
313 resulting ethyl hydroxybutyrate on a 7890A gas chromatograph (DB1-MS column, 100% dimethyl
314 polysiloxane, 15 m long, inner diameter 0.25 mm, film thickness 0.25 µm), with helium (5.0) as the
315 mobile phase at a flow rate of 1 mL min⁻¹, coupled to a 7000A triple quadrupole mass spectrometer
316 (all Agilent, Waldbronn, Germany). Injection volume was 1 µL at an inlet temperature of 270°C and
317 split ratio of 25:1. The GC temperature was: 42°C isothermal for 7 min; ramped to 77°C at 5°C min⁻¹;
318 then to 155°C at 15°C min⁻¹; held for 15 min; and the ramped to 200°C at 10°C min⁻¹. The transfer
319 line temperature was 280°C, with electron ionization at 70 eV. Quantification was based on ions at
320 m/z 43, 60 and 87 for the ethyl 3-hydroxybutyrate analyte, and at m/z 57, 71 and 85 for the
321 undecane internal standard. Identity and purity of peaks was confirmed by scan measurement
322 across the range m/z 40 to 300. The same chromatographic conditions were used for determination
323 of the PHB isotopic composition on a Thermo GC Isolink coupled with a Conflo IV interface to a MAT
324 253 isotope ratio mass spectrometer (all Thermo Fisher, Bremen, Germany), but with splitless
325 injection. The measured isotopic compositions were corrected for carbon added in derivatization
326 according Glaser and Amelung³⁷.

327 TAGs were extracted using established protocols for neutral and phospholipid analysis in soil ³⁸,
328 according to which lipids were first extracted from frozen soil into a single-phase chloroform-
329 methanol-water solution, purified by solvent extraction, and neutral lipids separated from more
330 polar lipids on a silica solid-phase extraction column. Following removal of the solvent by
331 evaporation, the purified TAGs were hydrolyzed (0.5 M NaOH in MeOH, 10 minutes at 100°C) and
332 methylated (12.5 M BF₃ in MeOH, 15 minutes at 85°C), followed by extraction into hexane, drying
333 and redissolution in toluene. The resulting fatty acid methyl esters were quantified by GC-MS on a
334 7890A gas chromatograph (DB-5 MS column, 5%-phenyl methylpolysiloxane, 30 m coupled to a DB1-
335 MS 15m long, both with an inner diameter 0.25 mm and film thickness 0.25 µm) with an injection
336 volume of 1 µl into the splitless inlet heated to 270°C, and at a constant flow of He (4.6) of 1.2 mL
337 min⁻¹, coupled to a 5977B series mass spectrometer (Agilent, Waldbronn, Germany), set to 70 eV
338 electron impact energy, with the GC oven programme as follows: initial temperature 80°C
339 isothermal for 1 min, ramped at 10°C min⁻¹ to 171°C, ramped at 0.7°C min⁻¹ to 196°C isothermal for 4
340 min, ramped at 0.5°C to 206°C, and ramped at 10°C min⁻¹ to the final temperature of 300°C,
341 isothermal for 10 min for column reconditioning. Isotopic composition was determined in triplicate
342 using a Trace GC 2000 (CE Instruments ThermoQuest Italia, S.p.A), coupled with a Combustion
343 Interface III to a DeltaPlus isotope-ratio mass spectrometer (Thermo Finnigan, Bremen, Germany)
344 using the same dimensions and parameters with splitless injection.

345 Growth was estimated by ¹⁸O incorporation into DNA^{10,11}. Parallel microcosms were prepared with
346 0.50 g soil in 2 mL Eppendorf tubes (Eppendorf, Hamburg, Germany) and incubated alongside the
347 larger microcosms. Treatment solutions were prepared at the same concentrations as for the larger
348 microcosms, but enriched with 97 atom% H₂¹⁸O so that addition provided a final soil solution of 4.2
349 atom% ¹⁸O. Tubes were withdrawn from incubation 24 h and 96 h after addition and immediately
350 frozen at -80°C. DNA was subsequently extracted using MP Bio FastDNA Spin Kit for Soil (MP
351 Biomedicals, Solon, OH, USA), following the manufacturer's recommendations. DNA concentration in
352 the extract was measured on an Implen MP80 nanophotometer (Implen, Munich, Germany) at 260
353 nm, with A260/280 and A260/A230 to confirm quality, and 50 µL was pipetted into silver capsules,
354 freeze dried, and measured by TC/EA (Thermo Finnigan, Bremen, Germany) coupled with a Conflo III
355 interface to a Delta V Plus isotope ratio mass spectrometer (all Thermo Finnigan, Bremen, Germany).
356 The total measured O content of the sample, the O content of the DNA (31 % by mass), and the ¹⁸O
357 natural abundance of unlabelled control samples were used to calculate the background ¹⁸O from
358 the kit. This background ¹⁸O was deducted to obtain ¹⁸O abundance of the DNA, which was applied in
359 a 2-pool mixing model with 70% of O in new DNA derived from water³⁹. This provided the fraction of

360 extracted DNA that had been newly synthesized during the incubation period. This fraction was
361 multiplied by extractable microbial biomass to arrive at gross biomass growth in units of $\mu\text{g C g}^{-1}$ soil.

362

363 3.3 Statistical analysis

364 Statistical analysis was performed in R⁴⁰. Dissolved nitrogen and DOC data was log-transformed to
365 satisfy assumptions for ANOVA (Shapiro-Wilk's test of normality and Levene's test for homogeneity
366 of variance), followed by Tukey's HSD test for pairwise comparisons of treatment effects. Where
367 relevant, effect sizes were computed as Cohen's d, using the effsize package⁴¹. The same analysis
368 was performed on untransformed extractable microbial biomass data.

369 Levels of labelled storage compounds showed considerable heteroskedasticity that could not be
370 consistently corrected by transformation, particularly due to very high levels of unsaturated fatty
371 acids in one of the 24 h samples. This conceivably reflected a hotspot of fungal activity in the soil.
372 This datapoint was therefore conservatively retained since this would comprise relevant variability in
373 the soil. Analysis of storage compounds proceeded by robust ANOVA of medians for each timepoint
374 separately using the R package WRS2⁴². Pairwise tests of median differences in storage (2-sided)
375 were calculated as 95% confidence intervals using the Hodges-Lehmann estimator (R package
376 DescTools⁴³).

377 Growth estimation by ¹⁸O incorporation used DNA concentration and its ¹⁸O enrichment to
378 determine mean gross microbial growth for each treatment in relative terms. The corresponding
379 mean extractable microbial biomass values were applied to convert to absolute units of $\mu\text{g C}$, using
380 standard rules of error propagation⁴⁴.

381 Results are presented as mean \pm standard deviation unless otherwise noted.

382

383 4 Acknowledgements

384 We gratefully acknowledge the laboratory assistance provided by Kali Middleby, Andrew Gall, Lydia
385 Köbele and Karin Schmidt. KMJ thanks the Deutscher Akademischer Austauschdienst (DAAD) for a
386 fellowship supporting the experimental work. This work is associated to the DFG Priority Program
387 2322 "SoilSystems", project EcoEnergeticS (DFG DI 2136/17-1). We thank the staff of the core
388 projects of the SPP and the scientific committee for establishing the SPP project.

389

390 5 Author contributions

391 KMJ, AB, CCB and MAD jointly initiated and designed the experiment; KMJ, AB and JD conducted the
392 experiment and analyses; KMJ and AB undertook data analysis; KMJ wrote the manuscript with
393 assistance and comments of all co-authors.

394

395 6 References

- 396 1. Sokol, N. W. *et al.* Life and death in the soil microbiome: how ecological processes influence
397 biogeochemistry. *Nat Rev Microbiol* (2022) doi:10.1038/s41579-022-00695-z.
- 398 2. Dijkstra, P. *et al.* High carbon use efficiency in soil microbial communities is related to balanced
399 growth, not storage compound synthesis. *Soil Biol. Biochem.* **89**, 35–43 (2015).
- 400 3. Geyer, K. M., Dijkstra, P., Sinsabaugh, R. & Frey, S. D. Clarifying the interpretation of carbon use
401 efficiency in soil through methods comparison. *Soil Biology and Biochemistry* **128**, 79–88 (2019).
- 402 4. Murphy, D. J. The dynamic roles of intracellular lipid droplets: From archaea to mammals.
403 *Protoplasma* **249**, 541–585 (2012).
- 404 5. López, N. I., Pettinari, M. J., Nikel, P. I. & Méndez, B. S. Polyhydroxyalkanoates: Much more than
405 biodegradable plastics. in *Advances in Applied Microbiology* vol. 93 73–106 (Elsevier, 2015).
- 406 6. Mason-Jones, K., Robinson, S. L., Veen, G. F., Manzoni, S. & van der Putten, W. H. Microbial
407 storage and its implications for soil ecology. *ISME J* (2021) doi:10.1038/s41396-021-01110-w.
- 408 7. Vance, E. D., Brookes, P. C. & Jenkinson, D. S. An extraction method for measuring soil microbial
409 biomass C. *Soil Biol. Biochem.* **19**, 703–707 (1987).
- 410 8. Anderson, J. P. E. & Domsch, K. H. A physiological method for the quantitative measurement of
411 microbial biomass in soils. *Soil Biol. Biochem.* **10**, 215–221 (1978).
- 412 9. Zelles, L., Bai, Q. Y., Rackwitz, R., Chadwick, D. & Beese, F. Determination of phospholipid- and
413 lipopolysaccharide-derived fatty acids as an estimate of microbial biomass and community
414 structures in soils. *Biol. Fertil. Soils* **19**, 115–123 (1995).

- 415 10. Blazewicz, S. J. & Schwartz, E. Dynamics of ^{18}O incorporation from H_2^{18}O into soil microbial DNA.
416 *Microb Ecol* **61**, 911–916 (2011).
- 417 11. Spohn, M., Klaus, K., Wanek, W. & Richter, A. Microbial carbon use efficiency and biomass
418 turnover times depending on soil depth – Implications for carbon cycling. *Soil Biology and*
419 *Biochemistry* **96**, 74–81 (2016).
- 420 12. Mason-Jones, K., Banfield, C. C. & Dippold, M. A. Compound-specific ^{13}C stable isotope probing
421 confirms synthesis of polyhydroxybutyrate by soil bacteria. *Rapid Commun. Mass Spectrom.* **33**,
422 795–802 (2019).
- 423 13. Bååth, E. The use of neutral lipid fatty acids to indicate the physiological conditions of soil fungi.
424 *Microb. Ecol.* **45**, 373–383 (2003).
- 425 14. Becker, K. W. *et al.* Daily changes in phytoplankton lipidomes reveal mechanisms of energy
426 storage in the open ocean. *Nat. Commun.* **9**, (2018).
- 427 15. Manzoni, S. & Porporato, A. Soil carbon and nitrogen mineralization: Theory and models across
428 scales. *Soil Biol. Biochem.* **41**, 1355–1379 (2009).
- 429 16. Wieder, W. R. *et al.* Explicitly representing soil microbial processes in Earth system models: Soil
430 microbes in Earth system models. *Global Biogeochem. Cycles* **29**, 1782–1800 (2015).
- 431 17. Chapin, F. S., Schulze, E. & Mooney, H. A. The ecology and economics of storage in plants. *Annu.*
432 *Rev. Ecol. Syst.* **21**, 423–447 (1990).
- 433 18. Matin, A., Veldhuis, C., Stegeman, V. & Veenhuis, M. Selective advantage of a *Spirillum* sp. in a
434 carbon-limited environment. Accumulation of poly- β -hydroxybutyric acid and its role in
435 starvation. *J. Gen. Microbiol.* **112**, 349–355 (1979).
- 436 19. Poblete-Castro, I. *et al.* The metabolic response of *P. putida* KT2442 producing high levels of
437 polyhydroxyalkanoate under single- and multiple-nutrient-limited growth: Highlights from a
438 multi-level omics approach. *Microb. Cell Fact.* **11**, 34 (2012).
- 439 20. Kourmentza, C. *et al.* Recent advances and challenges towards sustainable
440 polyhydroxyalkanoate (PHA) production. *Bioengineering* **4**, 55 (2017).

- 441 21. Gunina, A. & Kuzyakov, Y. Sugars in soil and sweets for microorganisms: Review of origin,
442 content, composition and fate. *Soil Biology and Biochemistry* **90**, 87–100 (2015).
- 443 22. Blagodatskaya, E. V., Blagodatsky, S. A., Anderson, T.-H. & Kuzyakov, Y. Priming effects in
444 Chernozem induced by glucose and N in relation to microbial growth strategies. *Applied Soil*
445 *Ecology* **37**, 95–105 (2007).
- 446 23. Schneckenberger, K., Demin, D., Stahr, K. & Kuzyakov, Y. Microbial utilization and mineralization
447 of [¹⁴C]glucose added in six orders of concentration to soil. *Soil Biology and Biochemistry* **40**,
448 1981–1988 (2008).
- 449 24. Creamer, C. A., Jones, D. L., Baldock, J. A. & Farrell, M. Stoichiometric controls upon low
450 molecular weight carbon decomposition. *Soil Biology and Biochemistry* **79**, 50–56 (2014).
- 451 25. Sekar, K. *et al.* Bacterial glycogen provides short-term benefits in changing environments. *Appl.*
452 *Environ. Microbiol.* **86**, e00049-20 (2020).
- 453 26. Dijkstra, P. *et al.* On maintenance and metabolisms in soil microbial communities. *Plant Soil*
454 (2022) doi:10.1007/s11104-022-05382-9.
- 455 27. Kalscheuer, R., Wältermann, M., Alvarez, H. & Steinbüchel, A. Preparative isolation of lipid
456 inclusions from *Rhodococcus opacus* and *Rhodococcus ruber* and identification of granule-
457 associated proteins. *Archives of Microbiology* **177**, 20–28 (2001).
- 458 28. Alvarez, H. M. Relationship between β -oxidation pathway and the hydrocarbon-degrading
459 profile in actinomycetes bacteria. *Int. Biodeterior. Biodegradation* **52**, 35–42 (2003).
- 460 29. Wieder, W. R. *et al.* Carbon cycle confidence and uncertainty: Exploring variation among soil
461 biogeochemical models. *Global Change Biology* **24**, 1563–1579 (2018).
- 462 30. Mooshammer, M., Wanek, W., Zechmeister-Boltenstern, S. & Richter, A. Stoichiometric
463 imbalances between terrestrial decomposer communities and their resources: Mechanisms and
464 implications of microbial adaptations to their resources. *Front. Microbiol.* **5**, (2014).

- 465 31. Wutzler, T., Zaehle, S., Schrumpf, M., Ahrens, B. & Reichstein, M. Adaptation of microbial
466 resource allocation affects modelled long term soil organic matter and nutrient cycling. *Soil*
467 *Biology and Biochemistry* **115**, 322–336 (2017).
- 468 32. Manzoni, S. *et al.* Intracellular Storage Reduces Stoichiometric Imbalances in Soil Microbial
469 Biomass – A Theoretical Exploration. *Front. Ecol. Evol.* **9**, 714134 (2021).
- 470 33. Ehlers, W., Werner, D. & Mähner, T. Wirkung mechanischer Belastung auf Gefüge und
471 Ertragsleistung einer Löss-Parabraunerde mit zwei Bearbeitungssystemen. *Journal of Plant*
472 *Nutrition and Soil Science* **163**, 321–333 (2000).
- 473 34. Xu, X., Thornton, P. E. & Post, W. M. A global analysis of soil microbial biomass carbon, nitrogen
474 and phosphorus in terrestrial ecosystems: Global soil microbial biomass C, N and P. *Global Ecol.*
475 *Biogeogr.* **22**, 737–749 (2013).
- 476 35. Manzoni, S., Taylor, P., Richter, A., Porporato, A. & Ågren, G. I. Environmental and stoichiometric
477 controls on microbial carbon-use efficiency in soils: Research review. *New Phytologist* **196**, 79–
478 91 (2012).
- 479 36. Gunina, A., Dippold, M. A., Glaser, B. & Kuzyakov, Y. Fate of low molecular weight organic
480 substances in an arable soil: From microbial uptake to utilisation and stabilisation. *Soil Biology*
481 *and Biochemistry* **77**, 304–313 (2014).
- 482 37. Glaser, B. & Amelung, W. Determination of ¹³C natural abundance of amino acid enantiomers in
483 soil: methodological considerations and first results. *Rapid Communications in Mass*
484 *Spectrometry* **16**, 891–898 (2002).
- 485 38. Banfield, C. C., Dippold, M. A., Pausch, J., Hoang, D. T. T. & Kuzyakov, Y. Biopore history
486 determines the microbial community composition in subsoil hotspots. *Biology and Fertility of*
487 *Soils* **53**, 573–588 (2017).
- 488 39. Pold, G., Domeignoz-Horta, L. A. & DeAngelis, K. M. Heavy and wet: The consequences of
489 violating assumptions of measuring soil microbial growth efficiency using the 18O water
490 method. *Elementa: Science of the Anthropocene* **8**, 069 (2020).

- 491 40. R Core Team. *R: A Language and Environment for Statistical Computing*. (R Foundation for
492 Statistical Computing, 2020).
- 493 41. Torchiano, M. *Effsize - A Package For Efficient Effect Size Computation*. (Zenodo, 2016).
494 doi:10.5281/ZENODO.1480624.
- 495 42. Mair, P. & Wilcox, R. Robust statistical methods in R using the WRS2 package. *Behav Res* **52**,
496 464–488 (2020).
- 497 43. Signorell, A. & et al. *DescTools: Tools for descriptive statistics*. (2021).
- 498 44. Meyer, S. L. *Data Analysis for Scientists and Engineers*. (John Wiley and Sons, 1975).
- 499
- 500
- 501